Author/s:
Hopkins, D;Callary, SA;Solomon, LB;Woodford, SC;Lee, PVS;Ackland, DC

Title:
Computational modeling of revision total hip arthroplasty involving acetabular defects: A systematic review

Date:
2024-10-01

Citation:
Hopkins, D., Callary, S. A., Solomon, L. B., Woodford, S. C., Lee, P. V. S. & Ackland, D. C. (2024). Computational modeling of revision total hip arthroplasty involving acetabular defects: A systematic review. Journal of Orthopaedic Research, 42 (10), pp.2249-2263. https://doi.org/10.1002/jor.25902.

Persistent Link:
https://hdl.handle.net/11343/351136

Received: 8 January 2024 | Revised: 22 April 2024 | Accepted: 7 May 2024
DOI: 10.1002/jor.25902

RESEARCH ARTICLE

Journal of Orthopaedic Research®

Computational modeling of revision total hip arthroplasty involving acetabular defects: A systematic review

Daniel Hopkins[1] | Stuart A. Callary[2,3] | L. B. Solomon[2,3] | Sarah C. Woodford[1] | Peter V. S. Lee[1] | David C. Ackland[1]

[1]Department of Biomedical Engineering, University of Melbourne, Parkville, Victoria, Australia

[2]Centre for Orthopaedic and Trauma Research, University of Adelaide, Adelaide, South Australia, Australia

[3]Department of Orthopaedics and Trauma, Royal Adelaide Hospital, Adelaide, South Australia, Australia

Correspondence
David C. Ackland, Department of Biomedical Engineering, University of Melbourne Parkville, VIC 3010, Australia.
Email: dackland@unimelb.edu.au

Funding information
Australian Research Council, Grant/Award Numbers: FT200100098, IC180100024; The Hospital Research Foundation Group

Abstract

Revision total hip arthroplasty (rTHA) involving acetabular defects is a complex procedure associated with lower rates of success than primary THA. Computational modeling has played a key role in surgical planning and prediction of postoperative outcomes following primary THA, but modeling applications in rTHA for acetabular defects remain poorly understood. This study aimed to systematically review the use of computational modeling in acetabular defect classification, implant selection and placement, implant design, and postoperative joint functional performance evaluation following rTHA involving acetabular defects. The databases of Web of Science, Scopus, Medline, Embase, Global Health and Central were searched. Fifty-three relevant articles met the inclusion criteria, and their quality were evaluated using a modified Downs and Black evaluation criteria framework. Manual image segmentation from computed tomography scans, which is time consuming, remains the primary method used to generate 3D models of hip bone; however, statistical shape models, once developed, can be used to estimate pre-defect anatomy rapidly. Finite element modeling, which has been used to estimate bone stresses and strains, and implant micromotion postoperatively, has played a key role in custom and off-the-shelf implant design, mitigation of stress shielding, and prediction of bone remodeling and implant stability. However, model validation is challenging and requires rigorous evaluation and comparison with respect to mid- to long-term clinical outcomes. Development of fast, accurate methods to model acetabular defects, including statistical shape models and artificial neural networks, may ultimately improve uptake of and expand applications in modeling and simulation of rTHA for the research setting and clinic.

KEYWORDS
acetabulum, biomechanical model, prosthesis, stability

1 | INTRODUCTION

Total hip arthroplasty (THA) is the established surgical procedure for the treatment of end-stage bone and joint conditions of the hip, including osteoarthritis, fracture and tumors. While THA has a 96% implant survival rate at 10 years,[1] up to 42% of implants are revised by 25 years.[2] The most common complications of THA are dislocation, fracture, infection and implant loosening, which often require revision THA (rTHA).[3] Acetabular bone defects are known to occur due osteolysis as a result of implant stress-shielding, infection, and rTHA,[4] limiting the amount and quality of bone for rTHA component fixation. Variation in shape, size and position of acetabular defects affects implant-bone contact in rTHA, with larger defects reducing the available contact area for implant fixation, which can result in increased implant micromotion and reduced potential for acetabular cup osseointegration. As a consequence, complication rates following rTHA in the presence of acetabular defects are over 5 times larger than those of primary THA.[5]

Computational modeling has gained popularity in rTHA involving acetabular defects as a tool for estimation of quantities that are difficult or impossible to measure non-invasively, including joint-contact force, implant stress, implant-bone strains and implant-bone micromotion.[6] This has led to improved classification of acetabular defects,[7,8] informed surgical planning of rTHA procedures,[9] and facilitated prediction of postoperative implant functional performance.[10,11] Strategies such 3D geometric bone modeling, musculoskeletal modeling of muscle and joint loads, and finite element analysis for prediction of joint and implant contact mechanics, have been widely applied in THA applications. This includes prediction of implant size and placement[12] and postoperative implant stability[13,14]; however, computational modeling of rTHA involving acetabular defects has received comparatively less attention to date, due primarily to the challenges in quickly, reliably and accurately delineating bone geometry from medical imaging. This is because imaging of the hip pre-rTHA is often heavily affected by metal artifact (Figure 1), and the underlying bony anatomy is markedly different to that in primary THA.

The aim of the present study was to systematically review methods for computational modeling of rTHA in the presence of acetabular defects, and describe how these techniques have been employed in defect classification, implant design, implant selection and placement, and assessment of implant functional performance. The findings of this study will be useful in supporting model-based decision making for improved clinical outcome of rTHA.

2 | METHODS

2.1 | Literature review strategy

A literature search was conducted to identify articles published up to April 10, 2023, on the following electronic databases: (1) Scopus, (2) MEDLINE, via Ovid, (3) EMBASE, via Ovid, (4) Web of Science, (5) CENTRAL database and (6) Global Health. The review was conducted in accordance with the Preferred Reporting Items for systematic reviews and Meta-Analyses (PRISMA) statement.[15] To ensure that the search captured as many relevant articles as possible, the following keywords were used:

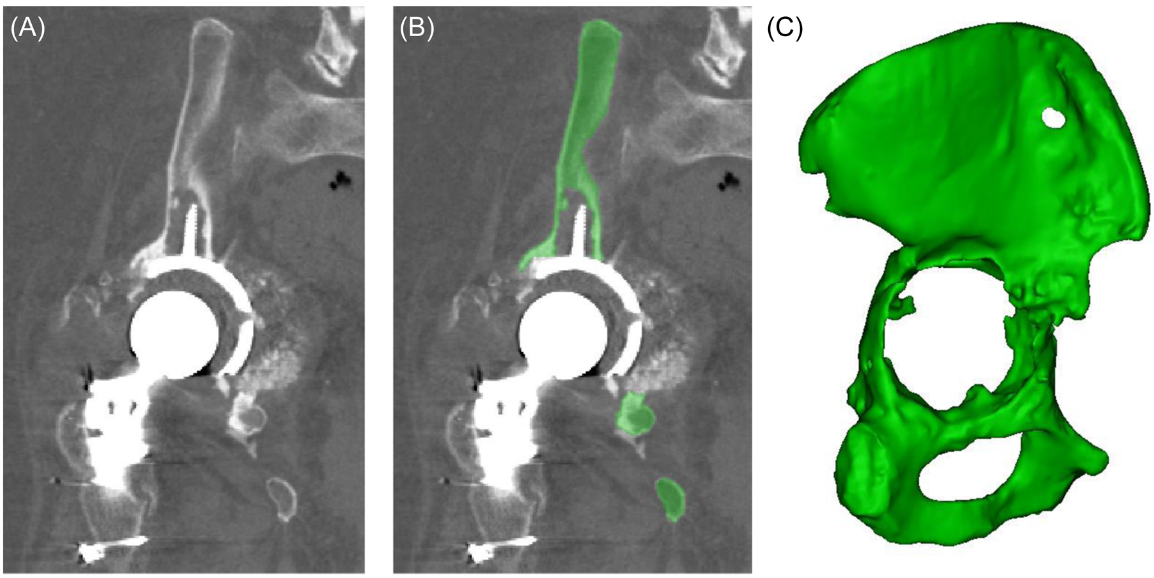

FIGURE 1 Illustration of 3D geometric bone model of pre-operative rTHA patient created from medical images including (A) CT images affected by metal artifact, (B) segmentation mask generated by manual annotation of CT images, and (C) virtual 3D geometric bone model created by digitally reconstructing segmentation mask.

- "acetabul*" AND
- "defect*" OR "deformit*" OR "lesion*" OR "osteoly*" AND
- "model*" OR "simulat*"

2.2 | Selection criteria

Once duplicate results were removed, all titles and abstracts of the remaining articles were screened by two reviewers (DH and SW) against the inclusion criteria. To be included, all articles had to: (i) be written in English Language, (ii) relate to THA involving acetabular defects, (iii) employ computational modeling. Exclusion criteria were: (i) animal studies, (ii) in vitro or in vivo studies, (iii) review articles, (iv) studies focused on manual segmentation from medical images. The reference sections of included articles were then checked for additional articles that may have been within the scope of the review (Figure 2).

2.3 | Quality assessment

A quality assessment tool was created using the established Downs and Black criteria,[16] STROBE checklist[17] and a previous systematic review.[18] The tool consisted of 10 questions scored using either 2, 1 or 0 corresponding to whether the question was clearly address, partially addressed, or not addressed, respectively (Table 1). A total score of ≥18 indicated high methodological quality, moderate quality was indicated by a score >12 and <18, while low quality was indicated by a score of ≤12. Scoring was separately assessed by two independent reviewers and discussion used to resolve conflicts (Tables 2–5).

3 | RESULTS

3.1 | Search and quality assessment results

A total of 2694 records were identified, and after removal of duplicates, 1243 records remained. The titles and abstracts were screened, resulting in 116 studies. The full texts of these studies were then assessed, resulting in 47 studies for inclusion. A further 6 studies were identified via bibliography screening. The mean methodological quality score was 13.7 with a range of 5 to 19. Nine studies were

TABLE 1 Quality assessment criteria employed in present study.

	Criteria
1.	Is the scientific background and rationale for the study clearly stated?
2.	Is the hypothesis/aim/objective of the study clearly described?
3.	Is the methodology of the study adequately described?
4.	Are the parameters to be measured clearly stated?
5.	Are the characteristics of the acetabular defects included in the study clearly described?
6.	Is patient inclusion and exclusion criteria clearly stated?
7.	Was the study cohort size sufficiently large that the results are applicable to the range of defects found in the population?
8.	Were the main outcome measures used accurate, valid, and reliable?
9.	Were study limitations or sources of bias considered?
10.	Are the main findings of the study clearly described?

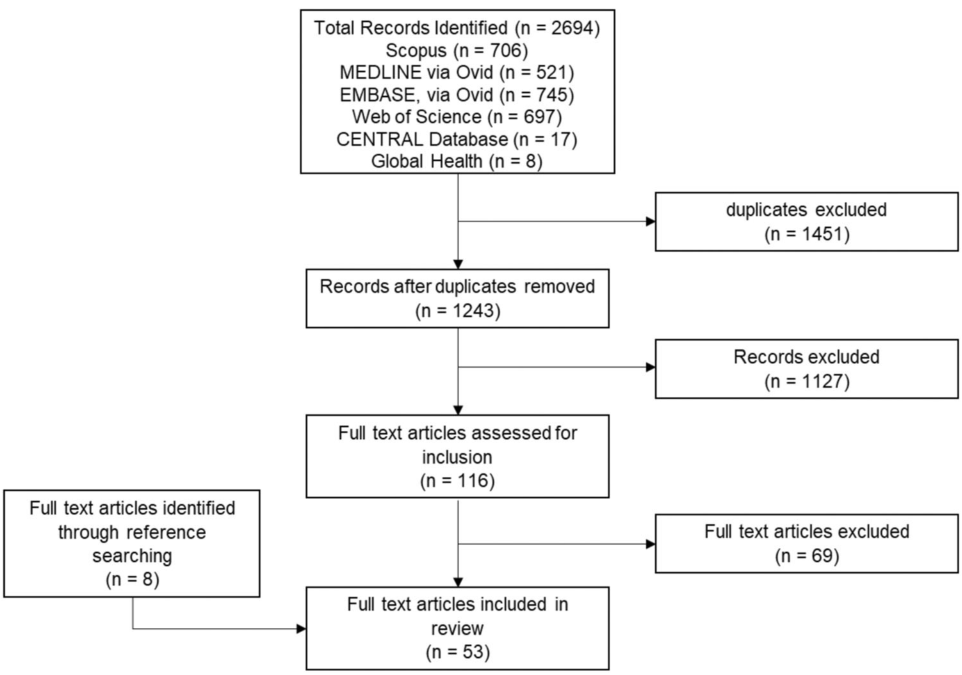

FIGURE 2 Flow chart illustrating systematic review screening process.

TABLE 2 Details of included studies that focus on anatomical reconstruction, including computational model outputs, defect classification system, defect type, computational method, software employed, and quality rating.

Authors	Model output	Defect classification system and defect type(s)	Computational method(s)	Software	Quality rating
Meynen et al.[27]	Defect and pre-defect anatomy	ADC, 1-4, Real	Manual segmentation, SSM	Mimics	12
Gelaude et al.[26]	Defect and pre-defect anatomy and bone loss ratio	Paprosky, IIIb and IIc, Real	Manual segmentation, SSM, custom algortihm	Mimics, MATLAB	18
Schierjott et al.[25]	Defect and pre-defect anatomy	Paprosky, IIa - IIIb and PD, Real	Manual segmentation, SSM	Mimics, 3-Matic, Geomagic, CATIA V5	18
Southwell et al.[19]	Defect detection zones via radiograph angle	N/A	CAD modeling, Radiograph simulation	AutoCAD	14
Otake et al.[20]	Simulated CT images with reduced metal artifact	Not classified, Artifical	Radiogrpah simulation	MATLAB	12
Grace et al.[24]	Defect volume and acetabular bone mineral density	Not classified, Artifical	Manual segmentation, custom algortihm	Mimics, MATLAB, NMSBuilder	18
Grace et al.[58]	Pelvic stress and strains	Not classified, Real	Manual segmentation, FEA	Mimics, 3matic	17
Vanden Berghe et al.[22]	Defect and pre-defect anatomy	Paprosky, IIa - IIIb, Artifical	Manual segmentation, SSM	Mimics, ACVD	18
Meynen et al.[23]	Defect and pre-defect anatomy	Not classified, Real	Manual segmentation, SSM	Mimics	17
Meynen et al.[21]	Defect and pre-defect anatomy	Paprosky, IIa - IIIb and PD, Artificial	Manual segmentation, SSM	Mimics, MATLAB, Scalismo	17
Hettich et al.[8]	Defect and pre-defect anatomy	Paprosky, IIIa, Real	Manual segmentation, SSM	Mimics, 3-Matic, Geomagic, CATIA V5	17

rated as high quality, 27 as moderate and 19 had a low-quality score. Most studies received low scores for questions 5, 6, 7 and 9 (Figure 3). Questions 5, 6 and 7 related to defect and cohort description and size, indicating that most studies had small sample sizes and did not adequately describe the characteristics of the defects studied. Question 9 considered the limitations and bias of the studies, and the low scores suggest many studies did not consider these adequately.

3.2 | Defect identification, reconstruction, and classification

One moderate quality study used digitally reconstructed radiographs from an implant CAD model to determine the optimal configuration of 2D radiographs to detect osteolysis immediately adjacent to the cup.[19] A low-quality study merged CT data and an implant CAD model to generate simulated radiographs affected by metal artifact.[20] Three different reconstruction algorithms were then tested and compared to the original CT data without metal artifact. A known component reconstruction algorithm utilising implant geometry and material data to estimate implant location and associated artifact, which could then be eliminated from the reconstruction, facilitated optimal visualisation of osteolytic regions.

Estimation of native pelvic anatomy in cases with existing acetabular defects has been achieved using statistical shape models (SSMs) (Figure 4). Two moderate quality papers found that the reconstruction error of specific anatomical features, such as hip joint centre (HJC) location, increased with defect size,[21,22] with pelvic discontinuities resulting in the largest errors in HJC location.[21] When estimating native anatomy in these cases, pathological bone anatomy was removed via boolean operations to ensure that only healthy anatomy influences the estimation; however, a moderate quality study found that bony reconstruction errors increased as larger volumes of the pathological bone were hidden, with irregular anatomy further increasing these errors.[8] A study of moderate quality used a ray-casting technique to compare native and defect anatomies and develop an SSM of the defects geometry.[23] The resulting SSM explained 85% of the defect anatomy variation using the first 10 modes, and the generalization error, a metric used to assess SSM performance, was 0.32 mm if all 86 modes were used. However, this model was not validated on unseen data. Another paper of high methodological quality developed a semi-automated segmentation pipeline to reconstruct defect anatomy and calculate lesion volume.[24] The method calculated lesion volume within a

TABLE 3 Details of studies that focus on implant design, including computational model outputs, defect classification system, defect type, computational method, software employed, and quality rating.

Authors	Model output	Defect classification system and defect type(s)	Computational method(s)	Software	Quality rating
Costin et al.[35]	Custom acetabular implant device	Paprosky, IIIa, Artificial	Manual segmentation, virtual 3D modeling, CAD	Geomagic	**9**
Sadovoy et al.[30]	Custom acetabular implant device	Not classified, Real	Manual segmentation. Virtual 3D modeling, CAD	InVesalius	**7**
Marinescu et al.[34]	Custom acetabular implant device	Paprosky, IIIa, Real	Manual segmentation, virtual 3D modeling, CAD	Mimics	**12**
Xiao et al.[32]	Custom acetabular implant device	Paprosky IIIb, Real	Manual segmentation, Virtual 3D modeling, Contralateral modeling, CAD	Mimics, Geomagic, Magics	**12**
Skalski et al.[36]	Custom acetabular implant device	Not classified, Real	Manual segmentation, CAD	Pro/Engineer	**8**
Costin et al.[31]	Custom acetabular implant device, implant stresses and deformation	Not classified, Real	Manual segmentation, Virtual 3D modeling, CAD, FEA	Slicer 4D, 3D Doctor, Geomagic, SolidWorks	**8**
Bartels et al.[33]	Custom acetabular implant device, implant and pelvic stresses, predicted muscle length changes	Paprosky, IIIb, Real	Manual segmentation, Virtual 3D modeling, CAD, FEA, Musculo-skeletal modeling		**10**
Dóczi et al.[51]	Custom acetabular implant device	Not classified, Real	Manual segmentation, Virtual 3D modeling, CAD	3D slicer, MeshMixer, SolidWorks	**10**
Zimmermann et al.[72]	Electric field strength	Paprosky IIC and PD, Artificial	FEA	CST EM studio	**14**
Potratz et al.[73]	Electric field strength	Not classified, real	CAD, FEA	Pro/Engineer, CST Studio	**10**
Potratz et al.[74]	Electric field strength	Not classified, Real	CAD, FEA	Pro/Engineer, Solidworks, CST Studio	**11**
Faizan et al.[29]	HJC location, screw trajectory and contact length	n/a	Manual segmentation, virtual 3D modeling	SOMA	**13**

maximum mean absolute error of 284 mm^3 and had high intra- and interoperative agreement.

One high-quality study compared segmented defect models with healthy pre-defect SSM models and proposed a new acetabular defect classification system comprising 17 defect types based on bone loss regions and thresholds.[25] The thresholds defined were 10%, 25% and 50% bone loss in the acetabular cranial roof, anterior column, posterior column and medial wall, though the clinical implications of these thresholds were not explored. Another high-quality study proposed a novel quantitative method to assess defect size. Native anatomy was estimated via SSM or contralateral modeling, and a ray-casting technique used to assess defect depth. This approach was employed to create bone defect maps and a bone loss ratio, defined as the ratio of defective acetabulum surface area to the reconstructed native acetabulum surface area.[26] A high quality study tested the reliability of SSM-based acetabular defect classification and found that using SSMs to estimate pre-defect native anatomy in conjunction with 3D geometric bone models, CT data and radiographs resulted in higher intra- and inter-agreement of defect classification compared to when SSM reconstructions were not used.[27]

3.3 | Acetabular implant design

Given the mature state of THA implant designs, the complication risk associated with new and clinically untested designs may outweigh potential health benefits.[28] Computational modeling can facilitate the testing of novel implant designs in silico, which may reduce prosthesis development times and costs, as well as prevent unforeseen complications. For example, one low quality study used 3D geometric bone modeling to show that a new eccentric cup

TABLE 4 Details of studies that focus on implant selection and placement, including computational model outputs, defect classification system, defect type, computational method, software employed, and quality rating.

Authors	Model output	Defect classification system and defect type(s)	Computational method(s)	Software	Quality rating
Nwankwo et al.[40]	HJC location and bone removal quantity	Not classified, Artificial	Manual segmentation, Virtual 3D modeling	SOMA 3.2	17
Shen et al.[41]	HJC location, implant incliniation and anteversion, implant/bone contact surface area	AAOS, I - III, Real	Manual segmentation, Virtual 3D modeling	Mimics, 3-Matic, magic	20
Li et al.[62]	Acetabular contact stress, pelvic displacement. Implant stress, micromotion and displacement,	Paprosky, III	Manual segmentation, Virtual 3D modeling, FEA	Mimics, Geomagic. Solidworks, ABAQUS	16
Zhang et al.[42]	Screw contact length and angular spread	Not classified, Artificial	Manual segmentation, Virtual 3D modeling	Mimics	17
Xiao et al.[61]	Acetabular stresses and implant micromotion	Not classified, Artificial	Manual segmentation, Virtual 3D modeling, FEA	Marc, Mimics	12
Bazlov et al.[38]	Defect anatomy	Paprosky, IIb - PD, Real	Manual segmentation, Virtual 3D modeling	RadiAnt DICOM Viewer, InVesalius 3.0, Netfabb	14
Zhang et al.[39]	Defect anatomy, 2D projection of 3D model	Not classified, Real	Manual segmentation, Virtual 3D modeling	Medraw PrintV1	15

design reduced HJC superior migration, and in the case of extra-large jumbo cups, provided more screw fixation options.[29] Recent advances in computational modeling and manufacturing techniques have also supported the creation of customized acetabular revision components that aim to precisely conform to the shape of a patient's existing bone defect.

Development of custom implants requires a patient anatomy-centric computational modeling pipeline (Figure 5). Most approaches start with manual segmentation of patient CT images to obtain a 3D geometric model of the bone and defect. 3D geometric bone modeling is then used to calculate anatomical parameters such as HJC, and CAD software used to design an implant and virtually integrate it into the model.[30] Calculation of HJC has been achieved via anatomical markers,[31] sphere-fitting algorithms,[35] contralateral modeling,[32] and SSMs.[33] Modeling pipelines have also employed 3D geometric bone models to determine optimal screw trajectories for implant fixation using material properties of the trabecular bone mapped from HU values,[33] bone thickness,[34] or on the basis of the judgement of a surgeon or biomedical engineer.[31,35,36] Custom screw guides for use in surgery have also been designed to support optimal screw insertion trajectory intaoperatively.[31,33] Implant performance can then be estimated using FE modeling, although only three studies to date have integrated FE analysis as part of an implant design process.[31,33,37]

3.4 | Implant selection and placement for revision total hip arthroplasty

3D geometric bone modeling has been employed in multiple studies to aid implant selection or to evaluate implant selection and placement postoperatively.[38-42] A moderate quality study employed models of historical rTHA procedures involving acetabular defects and reassessed the defects for surgical procedure and implant selection.[38] The findings suggested that in 80% of cases, the prescribed treatments would remain unchanged, although changes were more common in cases with Paprosky III defects. A second study compared 3D geometric bone models with radiographs to calculate bone stock thresholds that would be sufficient for implantation of a standard cup without an augment or a customized cage device.[39] Based on the analysis of CT data from 43 patients, 34 receiving hemispherical cups and 9 receiving cup-cage reconstructions, the study determined that an implant/bone contact line length greater than 16 mm and a contact angle greater than 25.5° when using a 70 mm hemispherical cup, visible on an AP pelvic radiograph, constituted sufficient bone stock for a standard hemispherical cup. Two studies of high quality investigated the influence of cup size on anatomical parameters such as HJC.[40,41] Both studies employed finite element bone models to simulate implantation of extra-large jumbo acetabular cups, commonly used in rTHA involving AD. They found that the HJC migrated superiorly as cup size increased. A moderate quality study used 3D geometric bone modeling to assess optimal screw trajectories of eccentric jumbo cups when implanted

TABLE 5 Details of studies that focus on implant functional performance, including computational model outputs, defect classification system, defect type, computational method, software employed, and quality rating.

Authors	Model output	Defect classification system and defect type(s)	Computational method(s)	Software	Quality Rating
Durand-Hill et al.[64]	Implant position	Paprosky, IIIb, Real	Manual segmentation, Virtual 3D modeling	Mimics, ScanIP, MeshLab	14
Baauw et al.[63]	Implant position	Paprosky, IIIa - IIIb, Real	Manual segmentation, Virtual 3D modeling		13
Weber et al.[65]	Implant position	Paprosky, IIIa - IIIb, Real	Manual segmentation, Virtual 3D modeling		19
Munro et al.[10]	Pelvic stress	Not classified, Real	Virtual 3D modeling, FEA	ImageJ, Cmiss	17
Munro et al.[52]	Pelvic stress	Not classified, Real	Manual segmentation, FEA	ImageJ, Cmiss	15
Fu et al.[55]	Pelvic and implant stresses	Paprosky, IIIa, Real	Manual segmentation, Virtual 3D modeling, CAD, FEA	Mimics, Creo, Geomagic, Ansys	11
Munro et al.[53]	Pelvic stress	Not classified, Real	Manual segmentation, FEA	ImageJ, Cmiss	18
Plessers et al.[57]	Implant and pelvic stresses	Paprosky, IIIb, Real and nonclassified, Artificial	Manual segmentation, Virtual 3D modeling, FEA	Mimics, 3-Matic, ABAQUS	14
Levine et al.[54]	Pelvic and implant stresses, implant displacement	Paprosky, IIc - IIIa, Artificial	Manual segmentation, Virtual 3D modeling, FEA	Geomagic, Unigraphics, PATRAN, ABAQUS	16
Amirouche et al.[60]	Pelvic stress	AAOS, I, Artificial	Manual segmentation, Virtual 3D modeling, FEA	3matic, Ansys	16
Zhao et al.[56]	Pelvic, bone graft and screw stresses	AAOS, I, Artificial	Manual segmentation, Virtual 3D modeling, FEA	Mimics, Magics, Hypermesh, Hyperview	15
Amirouche et al.[60]	Implant insertion force, displacement, micromotion and acetabular stress	Not classified, Artificial	Manual segmentation, Virtual 3D modeling, FEA		16
Liu et al.[48]	Implant and pelvic stresses, implant micromotion	Not classified, Artificial	Manual segmentation, Virtual 3D modeling, FEA	Marc	10
Dóczi et al.[59]	Bone graft density changes	Not classified, Real	Manual segmentation, CAD, FEA, Remodeling algorithm	Hypermesh, OptiStruct	9
Costin et al.[31]	Custom acetabular implant device, implant stresses and deformation	Not classified, Real	Manual segmentation, Virtual 3D modeling, CAD, FEA	Slicer 4D, 3D Doctor, Geomagic, SolidWorks	8
Bartels et al.[33]	Custom acetabular implant device, implant and pelvic stresses, predicted muscle length changes	Paprosky, IIIb, Real	Manual segmentation, Virtual 3D modeling, CAD, FEA, Musculo-skeletal modeling		10
Dóczi et al.[37]	Implant topology optimisation	Not classified, Real	Manual segmentation, CAD, FEA	Slicer 3D, MeshMixer, SolidWorks	12
Mantell et al.[46]	Implant stresses	Not classified, Artifical	FEA	ABAQUS	15
Burton et al.[44]	Implant stresses and fatigue life	Not classified, Artifical	FEA	SAP80, Microtab	14
Smuin et al.[47]	Implant stresses	Not classified, Artifical	FEA	ABAQUS	18
Kaku et al.[45]	Implant stresses	Not classified, Artifical	FEA	ANSYS	18
Grottoli et al.[75]	Implant stresses and displacement	Not classified, Real	FEA	ABAQUS	9

(Continues)

TABLE 5 (Continued)

Authors	Model output	Defect classification system and defect type(s)	Computational method(s)	Software	Quality Rating
Kawanabe et al.[43]	Implant stresses	Not classified, Artifical	FEA	n/a	**11**
Ma et al.[49]	Implant stresses	Not classified, Artificial	FEA	ANSYS	**13**
Ma et al.[50]	Implant stresses	Not classified, Artificial	FEA	ANSYS	**13**

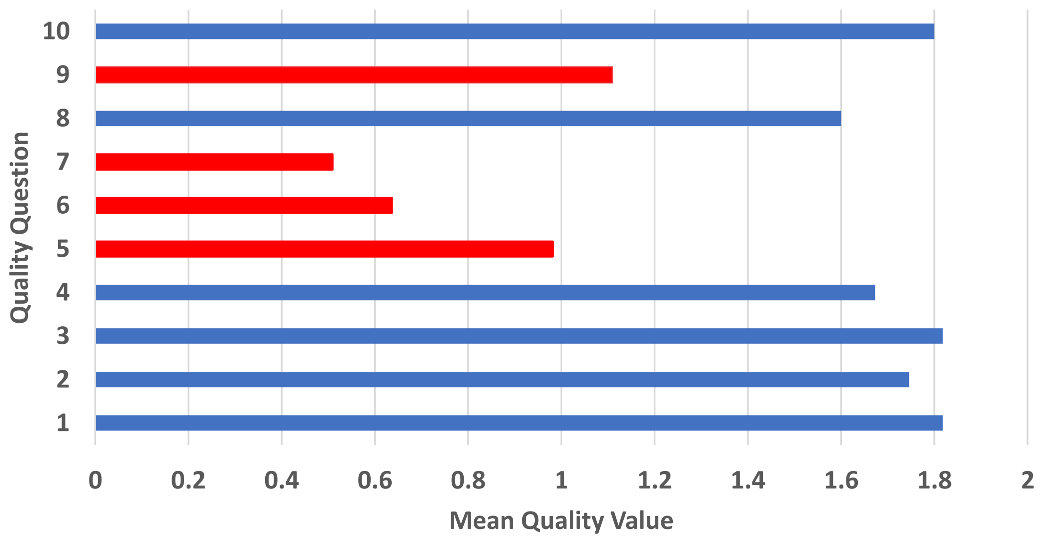

FIGURE 3 Mean quality assessment scores of included studies. Red bars indicate questions that were poorly addressed.

into healthy pelvises.[42] It was found that the angular spread of acceptable screw trajectories is independent of cup size (Figure 6).

3.5 | Quantifying implant functional performance

Postoperative implant functional performance after rTHA involving acetabular defects has been evaluated using FE modeling to estimate implant micromotion and bone stresses and strains as these are known to indicate the potential for osseointegration and therefore long-term implant stability (Figure 7). The load response of implants can also be evaluated using FE modeling, including estimates of implant displacement, and implant stresses and strains (Figure 8).

A low-quality study compared the stress response of four different acetabular reinforcement devices, finding that all devices reduced stresses in the acetabular cup compared to an acetabular cup without a reinforcement device.[43] Another low-quality study varied the loading conditions applied to a porous titanium cup to simulate different acetabular bone coverage and screw fixations. This study found that increasing bone support or screw fixation decreased implant stresses and increased implant fatigue life.[44] A third low quality study examined the load response of a custom acetabular device and found that an iterative design approach was required to mitigate excessive implant deformation and structural failure.[31]

A moderate quality study simulated defect zones as a 35 x 30 x 30 mm volume and showed that filling defects of increasing volume with bone grafts, in conjunction with Kerboull-type plate devices, reduced implant and screw stresses; however, these stresses increased with defect size, and trabecular bone grafts were associated with larger stresses in comparison to cortical bone grafts.[45] Two moderate quality studies modelled the acetabulum as a hemisphere and removed sections of the hemisphere to simulate reduced bone coverage as seen in cases of acetabular defects, while also varying implant configuration. One of these studies used a parametric design approach to show that the implant design variables with the largest influence on implant stresses were femoral head size and acetabular bone coverage of the acetabular cup.[46] Another study found that implant stresses were largest with smaller femoral heads and reduced bone coverage in standard, mono-block dual-mobility and modular dual-mobility cups.[47]

Modeling of artificially created defects in the superior acetabulum has been used to assess the mechanical behavior of winged implants. Three studies, two of moderate quality and one of low quality, showed that the use of wings on a hemispherical cup to fill superior acetabular defects in rTHA reduced implant stresses compared to unwinged hemispherical cups.[48-50] A moderate quality study performed a postoperative FE evaluation of a failed custom implant and found that material yield stresses were not exceeded,

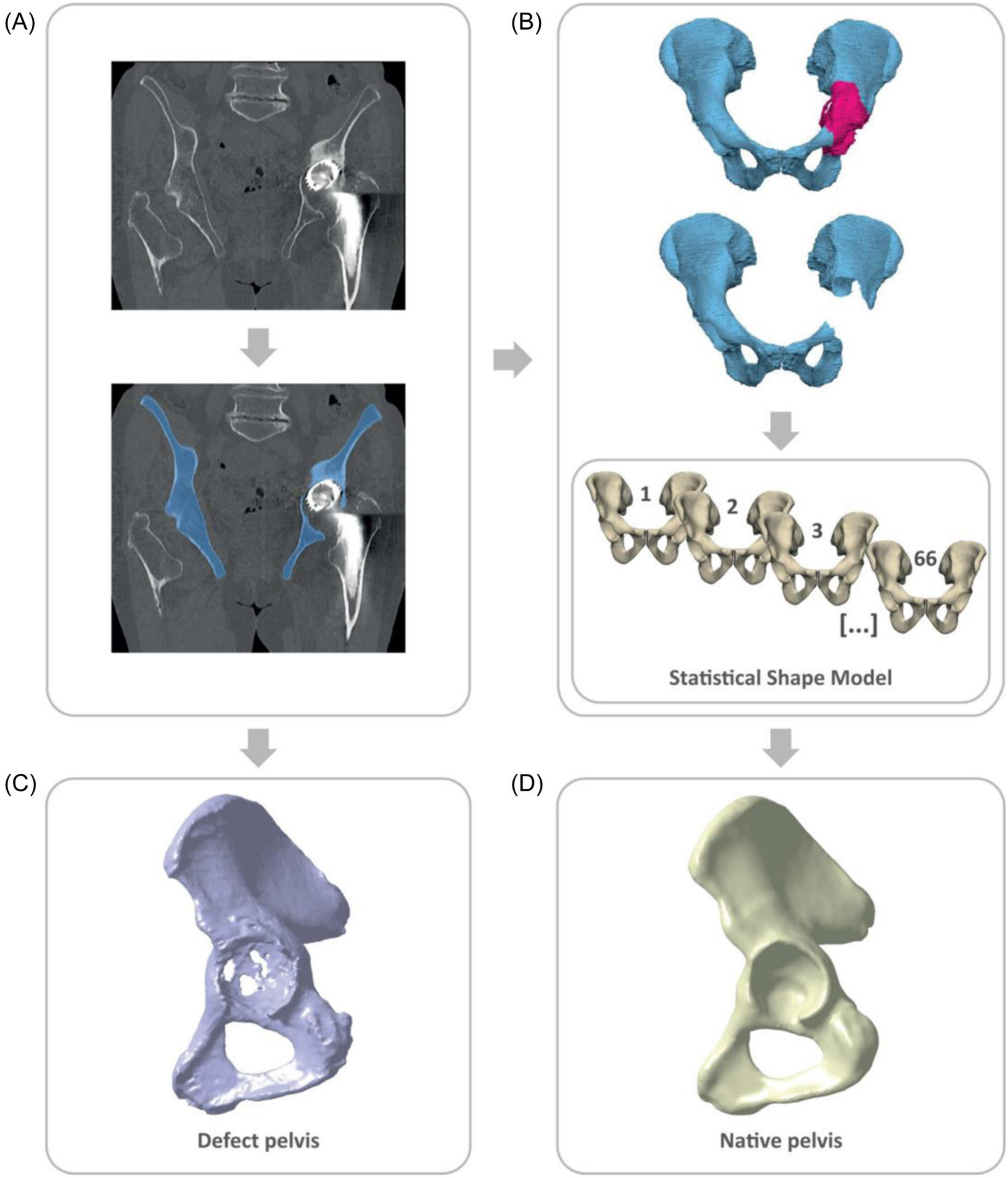

FIGURE 4 Example of statistical shape modeling including (A) segmentation of CT images, (B) creation of virtual 3D model with exclusion of defect areas, and input of remaining healthy anatomy into pre-calculated statistical shape model (SSM), (C) defect anatomy generation from segmentation mask, and (D) estimation of pre-defect anatomy by SSM. Adapted from Scherjott et al.[25]

though peak stresses calculated in a yielded screw suggested fatigue failure.[51]

Eight studies assessed postoperative pelvic loading after rTHA using FE modeling.[10,11,52-57] Four of these studies focused on small acetabular defects in which a standard acetabular cup could be implanted, with two high quality and one moderate quality study finding that the presence of small defects increased stresses in the acetabulum.[10,52,53] A moderate quality paper found that defects in the superior and inferior acetabular rim result in similar bone stresses to that in an intact rim when a cementless acetabular cup is used, and that defects of this type may not require additional augmentation.[11] The remaining four studies evaluated acetabular stresses when an augment or larger device was used to fill a large defect or holes in the medial wall.[54-57] A moderate quality study found that an augment or restrictor reduced acetabular bone stresses and increased implant stability.[54] This was in contrast to another moderate quality study which found stresses in periprosthetic bone remained higher than typical bone yield stresses when an augment was used.[55] Another

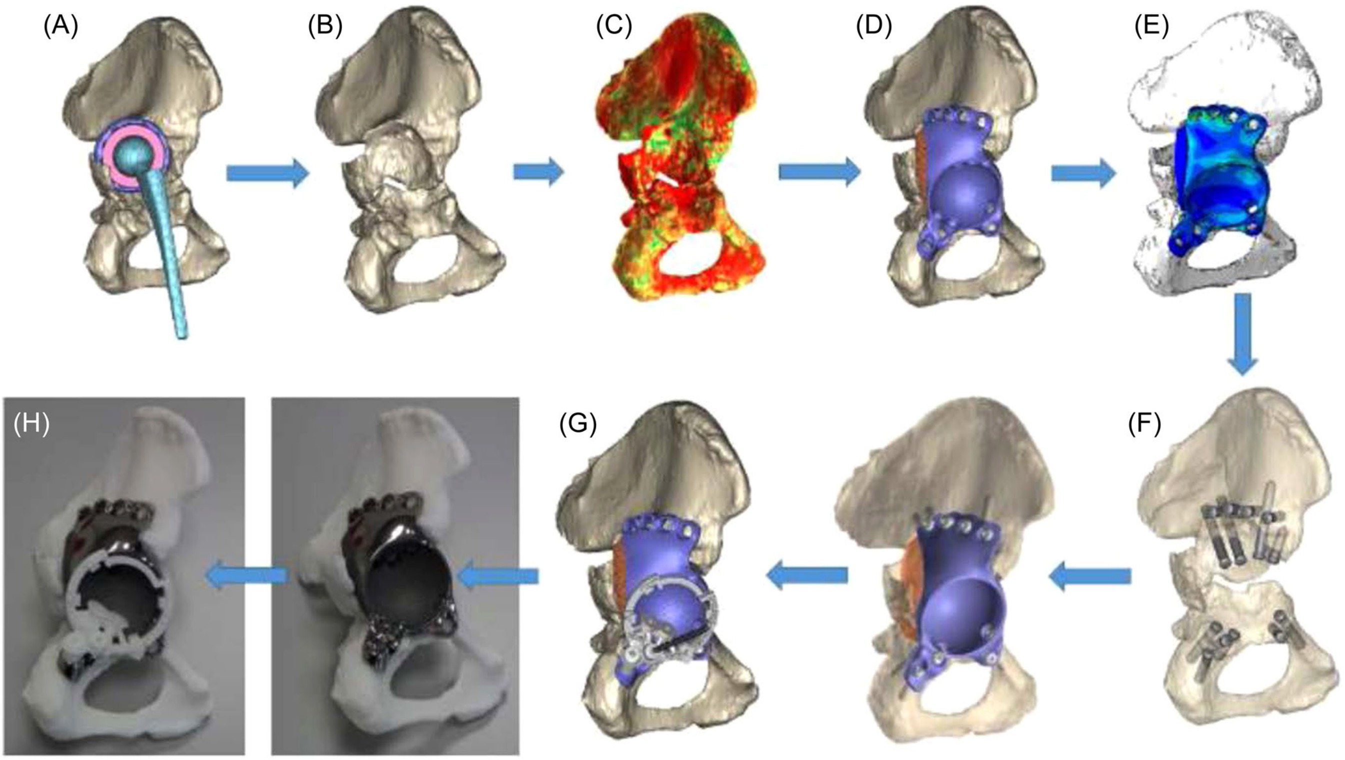

FIGURE 5 Custom implant design pipeline as described by Bartels et al.[33] which includes (A) preoperative view, (B) naked bone defect, (C) map of bone quality, (D) implant design, (E) FEA, (F) screw trajectory planning, (G) drill guide design, (H) manufactured implant and drill guide. Reprinted with permission from Springer Publishing.

FIGURE 6 Illustration of screw trajectories of an eccentric jumbo cup. Adapted from Zhang et al.[42]

moderate quality paper assessed bone grafts utilising a mortise-tenone joint, a joint commonly used in carpentry, and found that they reduced stresses in the acetabulum,[56] while a low-quality study found that acetabular stresses increased with defect size when a Burch-Schneider reinforcement cage was used in comparison to a healthy pelvis without an implant.[57]

One moderate quality FE modeling study assessed the results of differing acetabulum material property assignment approaches, finding that the mean strain results in the acetabular area were consistent across all strategies evaluated, although strain values in the superior acetabulum had a larger range than other regions.[58] A low-quality study investigated bone remodeling using adaptive FE modeling and a strain energy density based algorithm, with the authors estimating how the initial bone graft density affects change in bone density over time.[59] The study found that the rate of bone density change was similar for all initial bone densities.

Five studies used FE modeling to estimate primary stability indicators after rTHA for acetabular defects.[48,56,60-62] One moderate quality study compared cup displacement, rotation and micromotion when an artificial acetabular rim defect is present and the trabecular bone elastic modulus is varied.[60] The authors reported a decrease in implant stability as the bone elastic modulus was decreased, representing varying severities of osteoporosis, a condition

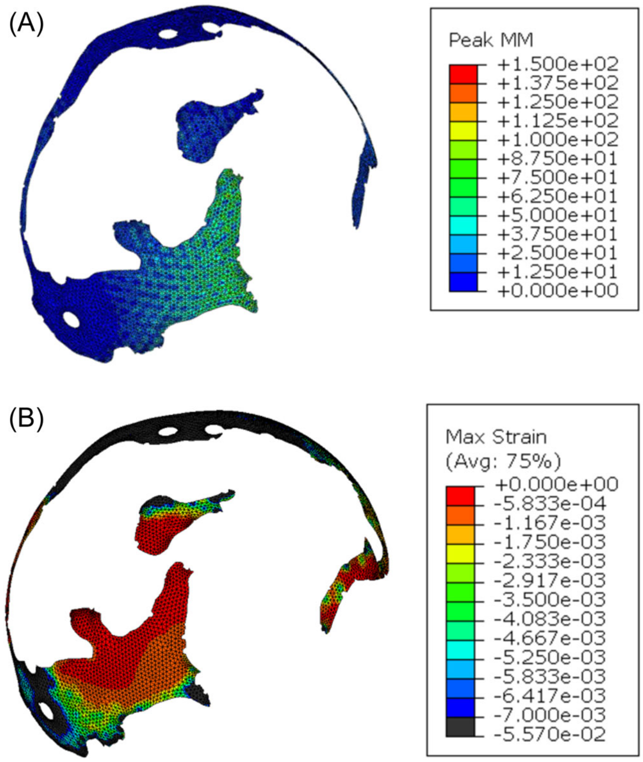

FIGURE 7 Postoperative acetabular distribution maps of (A) postoperative implant/bone micromotion, and (B) acetabular bone strains on a Paprosky IIIB acetabular defect reconstructed with an 80 mm jumbo cup and screws.

commonly seen in rTHA cases. Another moderate quality study found that the use of a mortise-tenone shaped bone graft reduced implant micromotion,[56] while a low quality study assessing implant micromotion of a winged implant found the wing angle had little effect on acetabular cup micromotion.[48] A low-quality study found that the screw configuration of a Ganz reinforcement ring had little effect on micromotion and the location of maximum stress[61] (Figure 6). Lastly, a study of moderate quality compared five different implant fixation methods and compared stress and micromotion values. The authors found that a 3-point fixation configuration into the pubis, ischium and superior acetabulum provided the lowest micromotion values and implant stress values closest to a primary THA press-fit cup.[62]

Three studies, one high quality and two moderate, used 3D geometric bone modeling to assess discrepancy in postoperative HJC, and acetabular inclination and anteversion from preoperative planned values.[63-65] The results showed the absolute mean deviations of HJC varied from ±4.8 to ±6.7 mm.

4 | DISCUSSION

The objective of this study was to systematically review computational modeling methods for rTHA in the presence of acetabular defects. Manual segmentation remains the established approach to reconstruct and delineate 3D geometric bone models of acetabular defects used for defect identification and classification, implant design, surgical

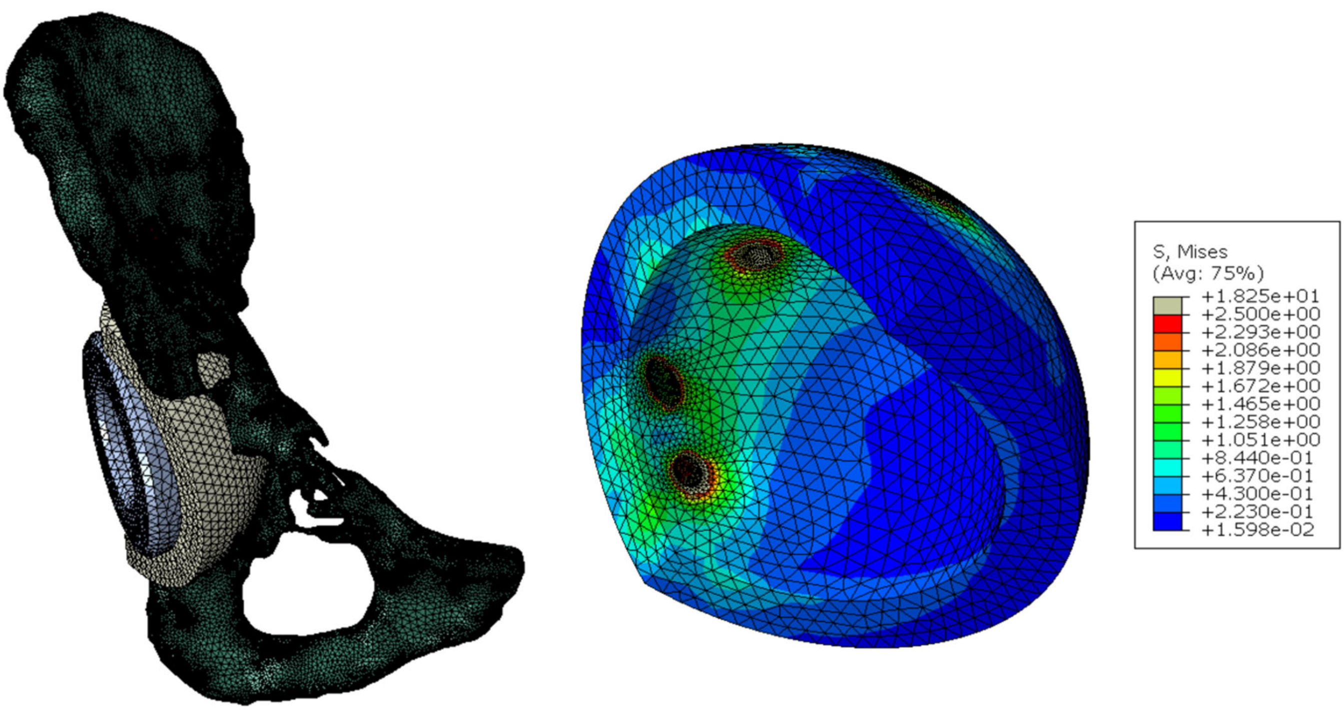

FIGURE 8 Example of an FEA model of hip joint loading following rTHA and the stress distribution computed at the acetabular cup.

planning, and biomechanical modeling of implant performance. Anatomical models derived from medical images are widely employed to investigate acetabular defects, perform preoperative surgical planning and support implant design; however, they are time consuming to produce, and may ultimately benefit from statistical shape modeling approaches to expedite bone shape generation. FE analysis has been used to estimate implant and bone mechanical performance assessment following rTHA, including implant micromotion and stress/strain response, but model development and simulation is highly time-consuming and requires considerable technical expertise, and is thus rarely performed on a subject-specific basis.

Statistical shape modeling is the most commonly used approach to quantify and classify acetabular defects. SSMs have been shown to improve inter- and intra-defect classification reliability compared to the Paprosky and AAOS clinical grading.[27] However, this approach does not currently allow accurate modeling of the defect itself. Meynen et al. (2020) developed a SSM based on defect anatomy from 87 patients, but its ability to estimate defect anatomy from incomplete anatomical data was not tested.[23] The large variations in defect anatomy that present clinically suggests that use of SSMs for 3D defect reconstruction requires a large non-homogenous training data set, which may be difficult or impossible to obtain. Grace et al. (2021) developed a semi-automated method for defect reconstruction, but this still relied on manual image segmentation,[24] Alternatively, image processing methods such as machine learning, including artificial neural networks, have been used to auto-segment and generate accurate bone models of healthy anatomy in seconds,[66] and may provide capability for automatic feature detection and defect classification; however, due to the requirement of large training datsets and challenges with metal artefact in medical images, these approaches have not yet been applied to pathological bone prior to rTHA.

3D geometric bone modeling has been adopted in preoperative planning to inform acetabular reconstruction,[38] determine postoperative HJC position,[29] calculate optimal location and trajectories of implant fixation screws,[42] and evaluate postoperative implant placement and alignment.[63-65] However, existing models have not incorporated the mechanical properties of bone or the response of the bone-implant fixation to physiological loading. The long-term integrity of an implant following THA involving acetabular defects is highly dependent on joint anatomy, implant selection and placement, as well as the underlying bone material properties. Furthermore, bone defect growth is driven, in part, by the mechanical behavior of periprosthetic bone, which is dependent on the physiological load environment. Finite element modeling approaches that combine 3D geometric bone modeling with implant and bone material behavior, have played a major role in our emerging understanding of implant stability following rTHA involving acetabular defects through calculation of implant micromotion. Computational modeling is currently the only known method for evaluating specific basis bone stress-strain behavior and implant micromotion non-invasively.

Implant micromotion has been directly measured in hip arthroplasty patients and used to evaluate implant fixation, with 150 µm identified as a threshold of allowable micromotion in which osseointegration occurs.[67] Subject-specific FE modeling has been used to estimate implant micromotion and implant stability post-rTHA, for example, linking increased bone-implant contact with lower micromotion,[62] or lower bone elastic modulus and unreconstructed superior defects to increase micromotion.[60,62] To achieve model validation, measurements of implant micromotion have been performed using sawbone testing and cadaveric experiments,[53,60] albeit for a limited range of implant configurations and loading scenarios. Reoentgenstereophotogrammetry analysis (RSA) has provided capability for radiographic measurement of implant micromotion in vivo,[68] with studies using micromotion measurements taken across multiple time points postoperatively to evaluate implant migration and stability. While this approach has primarily been adopted primarily in the setting of primary THA,[69] it is likely that mid- to long-term follow-up RSA data will play an increasing role in benchmarking for model predictions of implant micromotion following rTHA, and validation of FE model predictions of implant longevity. Recent advances in CT image processing have also allowed measurement of implant migration via CTMA (CT micromotion analysis), which unlike RSA, does not require the insertion of tantalum beads. The accuracy of CTMA has been shown to be 0.1–0.16 mm and 0.31–0.37°, which is comparative to RSA,[70] and this method could enable validation of FE models using even larger in vivo clinical datasets than those created from RSA studies. While RSA and CTMA provide capability to measure patient implant migration over time, cadaveric joint loading experiments using large-bore micro-CT can provide high-fidelity implant micromotion data for tasks such as walking and stair ambulation, though such tests are unable to evaluate the effect of osseointegration on implant stability.[71]

In practice, 3-point fixation in revision THA can be difficult to achieve due to defect and implant shape disparity, a lack of screw holes in standard acetabular cups, and obscured intra-operative vision of screw trajectories. 3D geometric bone modeling has been used to optimize screw trajectories to obtain fixation in the highest quality bone; however, the role of bone-screw contact on implant stability has not been explored in detail. In the future, automated modeling frameworks to provide implant selection and screw placement, and estimate functional performance and stability, may be achieved by combining automatic shape generation algorithms with screw placement algorithms, leveraging bone density and geometry data from CT scans. Such modeling frameworks, which could also be driven by artificial intelligence-based model generation, would require ease of use by a clinician or individual with minimal training, and be underpinned by rigorous validation.

End-to-end, computational modeling frameworks incorporating patient-specific anatomical reconstruction across a population, estimates of muscle and joint loading, implant design and selection, as well as virtual surgery, have potential to support large scale in silico trials. Such modeling, which in the future may be driven predominantly by artificial intelligence, could be used to evaluate the impact of new implant design and materials, surgical technique, defect type, joint load magnitude and rehabilitation on implant stability and longevity across a population. In silico virtual clinical trials across patient cohorts could ultimately reduce the speed and cost of clinical trials, support regulatory approval of new implantable components, and expedite the development of personalized joint replacement components.

This review has several limitations that ought to be discussed. Comparisons between studies reviewed, including meta-analysis, was not possible due to the inhomogeneous nature of the data reported. Assumptions made in model development, which were often unreported, include artefact reduction techniques used in image processing, material properties of pathological bone, and contact conditions between the periprosthetic bone and implant. These variables may ultimately have a substantial influence on model outputs, including model geometry, stress, strain and implant micromotion estimation.

Computational techniques are increasingly used in implant selection and design, preoperative planning, and postoperative implant stability prediction for rTHA involving acetabular defects. Manual segmentation, which remains the most commonly used and accurate method for defect reconstruction, is time intensive, challenging to perform, and represents the major bottleneck to patient-specific anatomical model development for rTHA. SSMs and artificial intelligence-driven approaches to defect reconstruction have demonstrated potential for rapid defect classification, and with the advent of larger datasets, are likely to play an increasing role in modeling of rTHA. FE modeling is the only approach available to predict load response of the hip following rTHA involving acetabular defects including estimation of implant micromotion and stress/strain response. Future directions to support greater model uptake in the research and clinical settings ought to consider user-friendly end-to-end frameworks to consolidate virtual defect reconstruction, surgical planning and implant load response estimation from medical images, as well as rigorous model validation using laboratory experiments, RSA and CTMA data.

AUTHOR CONTRIBUTIONS

Daniel Hopkins: Conception; data analysis and interpretation; paper writing. **Stuart A. Callary**: Data interpretation; proofing. **L. B. Solomon**: Data interpretation; proofing. **Sarah C. Woodford**: Data interpretation; proofing. **Peter V. S. Lee**: Funding; proofing. **David C. Ackland**: Funding; conception; proofing. All authors have read and approved the final submitted manuscript.

ACKNOWLEDGMENTS

This study was partially funded by an Australian Research Council Industry Transformation Training Centre (IC180100024),an Australian Research Council Future Fellowship to D.C.A. (FT200100098), and a Research Fellowship funded by The Hospital Research Foundation Group to S.A.C. Open access publishing facilitated by The University of Melbourne, as part of the Wiley - The University of Melbourne agreement via the Council of Australian University Librarians.

ORCID

Daniel Hopkins https://orcid.org/0009-0000-8094-3145
Stuart A. Callary https://orcid.org/0000-0002-2892-5238
L. B. Solomon https://orcid.org/0000-0001-6254-2372
Sarah C. Woodford https://orcid.org/0000-0003-4756-0198
David C. Ackland http://orcid.org/0000-0002-0559-7569

REFERENCES

1. Hunt LP, Whitehouse MR, Beswick A, et al. Implications of introducing new technology: comparative survivorship modeling of metal-on-metal hip replacements and contemporary alternatives in the National Joint Registry. *JBJS*. 2018;100(3):189-196.
2. Evans JT, Evans JP, Walker RW, Blom AW, Whitehouse MR, Sayers A. How long does a hip replacement last? A systematic review and meta-analysis of case series and national registry reports with more than 15 years of follow-up. *The Lancet*. 2019;393: 647-654.
3. Jafari MS, Coyle C, Mortazavi JSM, Sharkey PF, Parvizi J. Revision hip arthroplasty: infection is the most common cause of failure. *Clin Orthop Relat Res*. 2010;468:2046-2051.
4. Howie DW, Neale SD, Stamenkov R, et al. Progression of acetabular periprosthetic osteolytic lesions measured with computed tomography. *JBJS*. 2007;89(8):1818-1825.
5. Ong KL, Lau E, Suggs J, Kurtz SM, Manley MT. Risk of subsequent revision after primary and revision total joint arthroplasty. *Clin Orthop Relat Res*. 2010;468:3070-3076.
6. Mehta S, Tyler A, Hast M. Understanding the basics of computational models in orthopaedics: a nonnumeric review for surgeons. *J Am Acad Orthop Surg*. 2017;25:684-692.
7. Horas K, Arnholdt J, Steinert AF, Hoberg M, Rudert M, Holzapfel BM. Acetabular defect classification in times of 3D imaging and patient-specific treatment protocols. *Orthopade*. 2017;46:168-178.
8. Hettich G, Schierjott RA, Ramm H, et al. Method for quantitative assessment of acetabular bone defects. *J Orthop Res*. 2019;37: 181-189.
9. Di Laura A, Henckel J, Dal Gal E, Monem M, Moralidou M, Hart AJ. Reconstruction of acetabular defects greater than paprosky type 3B: the importance of functional imaging. *BMC Musculoskelet Disord*. 2021;22:207.
10. Munro JT, Millar JS, Fernandez JW, Walker CG, Howie DW, Shim VB. Risk analysis of patients with an osteolytic acetabular defect after total hip arthroplasty using subject-specific finite-element modelling. *Bone Joint J*. 2018;100B:1455-1462.
11. Amirouche F, Solitro GF, Walia A, Gonzalez M, Bobko A. Segmental acetabular rim defects, bone loss, oversizing, and press fit cup in total hip arthroplasty evaluated with a probabilistic finite element analysis. *Int Orthop*. 2017;41:1527-1533.
12. Huo J, Huang G, Han D, et al. Value of 3D preoperative planning for primary total hip arthroplasty based on artificial intelligence technology. *J Orthop Surg*. 2021;16:156.
13. O'Rourke D, Taylor M. Patient and surgical variability in the primary stability of cementless acetabular cups: a finite element study. *J Orthop Res*. 2020;38:1515-1522.
14. Bahl JS, Arnold JB, Saxby DJ. The effect of surgical change to hip geometry on hip biomechanics after primary total hip arthroplasty. *J Orthop Res*. 2023;41:1240-1247.
15. Moher D, Liberati A, Tetzlaff J, Altman DG. Preferred reporting items for systematic reviews and meta-analyses: the PRISMA statement. *BMJ*. 2009;339:b2535.
16. Downs SH, Black N. The feasibility of creating a checklist for the assessment of the methodological quality both of randomised and non-randomised studies of health care interventions. *J Epidemiol Community Health*. 1998;52:377-384.
17. von Elm E, Altman DG, Egger M, Pocock SJ, Gøtzsche PC, Vandenbroucke JP. The strengthening the reporting of observational studies in epidemiology (STROBE) statement: guidelines for reporting observational studies. *Ann Intern Med*. 2007;147:573-577.
18. Woodford SC, Robinson DL, Mehl A, Lee PVS, Ackland DC. Measurement of normal and pathological mandibular and temporomandibular joint kinematics: a systematic review. *J Biomech*. 2020;111:109994.

19. Southwell DG, Bechtold JE, Lew WD, Schmidt AH. Improving the detection of acetabular osteolysis using oblique radiographs. *J Bone Joint Surg Br*. 1999;81:289-295.
20. Otake Y, Stayman JW, Zbijewski W, et al. Model-based cone-beam CT reconstruction for image-guided minimally invasive treatment of hip osteolysis. Proceedings of SPIE 8671, Medical Imaging 2013: Image-Guided Procedures, Robotic Interventions, and Modeling, 86710Y, March 12, 2013. 2013. https://doi.org/10.1117/12.2008094. 2013.
21. Meynen A, Matthews H, Nauwelaers N, Claes P, Mulier M, Scheys L. Accurate reconstructions of pelvic defects and discontinuities using statistical shape models. *Comput Methods Biomech Biomed Engin*. 2020;23:1026-1033.
22. Vanden Berghe P, Demol J, Gelaude F, Vander Sloten J. Virtual anatomical reconstruction of large acetabular bone defects using a statistical shape model. *Comput Methods Biomech Biomed Engin*. 2017;20:577-586.
23. Meynen A, Vles G, Zadpoor AA, Mulier M, Scheys L. The morphological variation of acetabular defects in revision total hip arthroplasty-a statistical shape modeling approach. *J Orthop Res*. 2021;39:2419-2427.
24. Grace TM, O'Rourke D, Robertson T, et al. A semiautomated method to quantitatively assess osteolytic lesion volume and bone mineral density within acetabular regions of interest from CT. *J Orthop Res*. 2022;40:396-408.
25. Schierjott RA, Hettich G, Graichen H, et al. Quantitative assessment of acetabular bone defects: a study of 50 computed tomography data sets. *PLoS One*. 2019;14:e0222511.
26. Gelaude F, Clijmans T, Delport H. Quantitative computerized assessment of the degree of acetabular bone deficiency: total radial acetabular bone loss (TrABL). *Adv Orthop*. 2011;2011:1-12.
27. Meynen A, Vles G, Roussot M. Advanced quantitative 3D imaging improves the reliability of the classification of acetabular defects. *Arch Orthop Trauma Surg*. 2022;143:1611-1617.
28. Marc JN, Nelissen RGHH, Schoones JW, et al. Appraisal of evidence base for introduction of new implants in hip and knee replacement: a systematic review of five widely used device technologies. *BMJ*. 2014;349:g5133.
29. Faizan A, Black BJ, Fay BD, Heffernan CD, Ries MD. Comparison of head center position and screw fixation options between a jumbo cup and an offset center of rotation cup in revision total hip arthroplasty: a computer simulation study. *J Arthroplasty*. 2016;31:307-311.
30. Sadovoy MA, Pavlov VV, Bazlov VA, et al. Modeling of 3D implants via personalized contour correction with evaluation of bone tissue density on the hounsfield scale. *Biomed Eng*. 2018;52:195-198.
31. Costin S, Micu CA, Cristea S, et al. Process for realisation of a cage adapted to patient for specific acetabular defects in tha revision. UPB scientific bulletin. *UPB Sci Bull*. 2014;76:181-192.
32. Xiao C, Zhang S, Gao Z, et al. Custom-made 3D-printed porous metal acetabular composite component in revision hip arthroplasty with paprosky type III acetabular defects: A case report. *Technol Health Care*. 2022;31:283-291.
33. Bartels W, Gelaude F, Delport H, Jonkers I, Vander Sloten J. Patient-specific reconstruction of large bone defects: clinical success due to an integrated bioengineering workflow. In: Kyriacou E, Christofides S, Pattichis C. eds. *XIV Mediterranean Conference on Medical and Biological Engineering and Computing* 2016. IFMBE Proceedings, Vol 57. Springer. doi:10.1007/978-3-319-32703-7_127
34. Marinescu R, Popescu D. Additively manufactured customized implant for severe acetabular bone defect—a case report. International Conference on eȐHealth and Bioengineering (EHB), Lasi, Romania. 2021:1-4. doi:10.1109/EHB52898.2021.9657682
35. Costin S, Micu CA. Design and manufacturing preparation of a patient specific acetabular cage. *Adv Mater Res*. 2013;837:328-333.
36. Skalski K, Kwiatkowski K, Domanski J, Sowinski T. Computer-aided reconstruction of hip joint in revision arthroplasty. *J Orthop Traumatol*. 2006;7:72-79. doi:10.1007/s10195-006-0124-y
37. Dóczi MO, Sződy R, Zwierczyk PT. Effect of the design constraints and the loading model on the geometry of topology optimized acetabular cages. periodica polytechnica. *Mech Eng*. 2022;66:253-259.
38. Bazlov VA, Mamuladze TZ, Golenkov OI, et al. Effects of 3D imaging on surgical tactics in primary and revision hip arthroplasty. *Traumatology and Orthopedics of Russia*. 2020;26:60-70.
39. Zhang JW, Kong KY, Chi YJ, et al. Evaluation of the feasibility of acetabular cup pre-determination in revision total hip arthroplasty via x-ray of the bone stock of the anterosuperior acetabulum. *J Orthop Surg*. 2021:16.
40. Nwankwo C, Dong NN, Heffernan CD, Ries MD. Do jumbo cups cause hip center elevation in revision THA? A computer simulation. *Clin Orthop Relat Res*. 2014;472:572-576.
41. Shen X, Tian H, Li Y, Zuo J, Gao Z, Xiao J. Acetabular revision arthroplasty based on 3-dimensional reconstruction technology using jumbo cups. *Front Bioeng Biotechnol*. 2022;10:10.
42. Zhang Y, Ma H, Liu Y, Shen J, Zhang B, Zhou Y. The optimal screw-hole positions of the eccentric revision cup based on a morphological study. *J Orthop Surg*. 2022;17:386.
43. Kawanabe K, Akiyama H, Goto K, Maeno S, Nakamura T. Load dispersion effects of acetabular reinforcement devices used in revision total hip arthroplasty. *J Arthroplasty*. 2011;26:1061-1066.
44. Burton DS, Skinner HB. Stress analysis of a total hip acetabular component: an fem study. *Biomater Artif Cells Artif Organs*. 1989;17:371-383.
45. Kaku N, Hara K, Tabata T, Tsumura H. Influence of the volume of bone defect, bone grafting methods, and hook fixation on stress on the Kerboull-type plate and screw in total hip arthroplasty: three-dimensional finite element analysis. *Eur J Orthop Surg Traumatol*. 2015;25:321-329.
46. Mantell SC, Chanda H, Bechtold JE, Kyle RF. A parametric study of acetabular cup design variables using finite element analysis and statistical design of experiments. *J Biomech Eng*. 1998;120:667-675.
47. Smuin DM, Tucker SM, Rothermel SD, Lewis GS, Mason M. Effect of bone coverage on acetabular implant stresses in standard and dual-mobility total hip arthroplasty constructs: a finite element model. *Orthopedics*. 2021;44:280-284.
48. Liu YZ, Hai Y, Zhao H. Three-fin acetabular prosthesis for superior acetabular bone defects: a three-dimensional finite element analysis. *Chin Med J*. 2012;125:901-905.
49. Ma W, Zhang X, Wang J, Zhang Q, Chen W, Zhang Y. Optimized design for a novel acetabular component with three wings. A study of finite element analysis. *J Surg Res*. 2013;179:78-86.
50. Ma WH, Zhang XM, Zhang YZ. The comparative analysis of a novel acetabular component against hemispherical component in case of extensive acetabular bone defects—a study of finite element analysis. *Int J Adv Robot Syst*. 2013:10(2):1.
51. Dóczi MO, Zwierczyk PT, Szody R. Failure analysis of a custom-made acetabular cage with finite element method. *Proceedings—European Council for Modelling and Simulation, ECMS*. 2020;34:250-255.
52. Munro JT, Fernandez JW, Millar JS, et al. Altered load transfer in the pelvis in the presence of periprosthetic osteolysis. *J Biomech Eng-T ASME*. 2014:136(11).
53. Munro JT, Anderson IA, Walker CG, Shim VB. Finite element analysis of retroacetabular osteolytic defects following total hip replacement. *J Biomech*. 2013;46:2529-2533.
54. Levine DL, Dharia MA, Siggelkow E, et al. Repair of periprosthetic pelvis defects with porous metal implants: a finite element study. *J Biomech Eng-T ASME*. 2010;132(2):021006.
55. Fu J, Ni M, Chen J, et al. Reconstruction of severe acetabular bone defect with 3D printed Ti6Al4V augment: a finite element study. *BioMed Res Int*. 2018;2018:1-8.

56. Zhao X, Xue H, Sun Y, et al. Application of novel design bone grafting for treatment of segmental acetabular rim defects during revision total hip arthroplasty. *J Bionic Eng*. 2021;18:1369-1377.
57. Plessers K, Mau H. Stress analysis of a Burch-Schneider cage in an acetabular bone defect: a case study. *Reconstr Rev*. 2016;6:6.
58. Grace TM, Solomon LB, Atkins GJ, Thewlis D, Taylor M. Assigning trabecular bone material properties in finite element models simulating the pelvis before and after the development of periprosthetic osteolytic lesions. *J Mech Behav Biomed Mater*. 2022;133:105311.
59. Dóczi MO, Zwierczyk PT, Sződy R. Implementation of bone graft adaptation's FE model in hypermesh. *Proceedings—European Council for Modelling and Simulation, ECMS*. 2021;35:152-156.
60. Amirouche F, Solitro G, Broviak S, Goldstein W, Gonzalez M, Barmada R. Primary cup stability in THA with augmentation of acetabular defect. *Orthop Traumatol Surg Res*. 2015;101:667-673.
61. Xiao J, Zhao X, Wang Y, et al. Application of acetabular reinforcement ring with hook for correction of segmental acetabular rim defects during total hip arthroplasty revision. *J Bionic Eng*. 2018;15:154-159.
62. Li P, Tang H, Liu X, et al. Reconstruction of severe acetabular bone defects with porous metal augment in total hip arthroplasty: a finite element analysis study. *Proc Inst Mech Eng [H]*. 2021;236:9544119211052377.
63. Baauw M, van Hellemondt GG, van Hooff ML, Spruit M. The accuracy of positioning of a custom-made implant within a large acetabular defect at revision arthroplasty of the hip. *Bone Joint J*. 2015;97-B:780-785.
64. Durand-Hill M, Henckel J, Di Laura A, Hart AJ. Can custom 3D printed implants successfully reconstruct massive acetabular defects? A 3D-CT assessment. *J Orthop Res*. 2020;38:2640-2648.
65. Weber M, Witzmann L, Wieding J, Grifka J, Renkawitz T, Craiovan B. Customized implants for acetabular paprosky III defects may be positioned with high accuracy in revision hip arthroplasty. *Int Orthop*. 2019;43:2235-2243.
66. González Sánchez JC, Magnusson M, Sandborg M, Carlsson Tedgren Å, Malusek A. Segmentation of bones in medical dual-energy computed tomography volumes using the 3D U-Net. *Phys Med*. 2020;69:241-247.
67. Pilliar RM, Lee JM, Maniatopoulos C. Observations on the effect of movement on bone ingrowth into porous-surfaced implants. *Clin Orthop Relat Res*. 1986;208:108-113.
68. Solomon LB, Abrahams JM, Callary SA, et al. The stability of the porous tantalum components used in revision THA to treat severe acetabular defects: a radiostereometric analysis study. *JBJS*. 2018;100(22):1926-1933.
69. Fallahnezhad K, Callary SA, O'Rourke D. Corroboration of coupled musculoskeletal model and finite element predictions with in vivo RSA migration of an uncemented acetabular component. *J Orthop Res*. 2024;42:373-384.
70. Brodén C, Sandberg O, Olivecrona H, Emery R, Sköldenberg O. Precision of CT-based micromotion analysis is comparable to radiostereometry for early migration measurements in cemented acetabular cups. *Acta Orthop*. 2021;92:419-423.
71. Sukjamsri C, Geraldes DM, Gregory T, et al. Digital volume correlation and micro-CT: an in-vitro technique for measuring full-field interface micromotion around polyethylene implants. *J Biomech*. 2015;48:3447-3454.
72. Zimmermann U, van Rienen U. Identification of widely applicable configurations for the electrostimulative total hip revision system. *2012 Annual International Conference of the IEEE Engineering in Medicine and Biology Society*. 2012. doi:10.1109/embc.2012.6346607
73. Potratz C, Souffrant R, Bader R, Mittelmeier W, van Rienen U. Electrostimulation of bone defects in total hip revision in triple layered domains. World Congress on Medical Physics and Biomedical Engineering, September 7-12, 2009, Munich, Germany. 2009:2099-2102. doi:10.1007/978-3-642-03882-2_557
74. Potratz C, Glock H-W, Souffrant R, Bader R, Ewald H, van Rienen U. Periprosthetic fields and currents of an electrostimulative acetabular revision system. 4th European Conference of the International Federation for Medical and Biological Engineering 2009:1808-1811. doi:10.1007/978-3-540-89208-3_431
75. Grottoli CF, Cingolani A, Zambon F, Ferracini R, Villa T, Perale G. Simulated performance of a xenohybrid bone graft (SmartBone®) in the treatment of acetabular prosthetic reconstruction. *J Funct Biomater*. 2019;10(4):53. doi:10.3390/jfb10040053

How to cite this article: Hopkins D, Callary SA, Solomon LB, Woodford SC, Lee PVS, Ackland DC. Computational modeling of revision total hip arthroplasty involving acetabular defects: a systematic review. *J Orthop Res*. 2024;42:2249-2263. doi:10.1002/jor.25902